Retrieval of cloud optical properties using simple approximations: SLALOM

Thomas Nauss[a,*], Alexander A. Kokhanovsky[b]

[a]*Department of Geosciences, Bayreuth University, 95440 Bayreuth, Germany*
[b]*Institut of Environmental Physics, Bremen University, O. Hahn Allee 1, 28334 Bremen, Germany*

Abstract

A new technique relying on SimpLe Approximations for cLOudy Media (SLALOM) for the retrieval of cloud optical and microphysical parameters from optical satellite data during daytime is introduced. The technique is based on simple yet highly accurate approximations of the asymptotic solutions of the radiative transfer theory which have already been implemented in the forward radiative transfer model CLOUD. These approximations enable a solution of the equations of the corresponding backward model during runtime leading to a very fast computation speed. Since these asymptotic solutions are generally applicable to weakly absorbing media only, pre-calculated look-up tables for the reflection function of a semi-infinite cloud (and also the escape function) are used to overcome this restriction within this new retrieval. SLALOM is capable to retrieve the cloud optical thickness, the effective cloud droplet radius, the liquid and ice water paths, the particle absorption length as well as some other properties of water and ice clouds. The comparison of SLALOM with both exact radiative transfer computations and the NASA MODIS cloud property product shows a very good agreement. A Fortran implementation of both CLOUD and SLALOM is available for download under the Creative Commons Attribution-Noncommercial-Share Alike 3.0 license (see http://creativecommons.org/licenses/by-nc-sa/3.0) at http://www.klimatologie.uni-bayreuth.de.

Keywords: satellite retrieval, cloud properties, radiative transfer

1. Introduction

Clouds play an important role in the atmospheric radiation budget and are recognized as a key modifier of climate((Platnick and Valero, 1995)). Consequently, the Intergovernmental Panel on Climate Change (IPCC) has called for more measurements on cloud properties (Houghton et al., 2001). In addition, information on optical and microphysical cloud properties forms the basis of the most recent rainfall retrieval techniques that have been developed for optical satellite sensors (e. g. Nauss and Kokhanovsky, 2006; Lensky and Rosenfeld, 2006; Nauss and Kokhanovsky, 2007; Thies et al., 2008; Roebeling and Holleman, 2009; Kühnlein et al., 2010).

Many authors have developed techniques for cloud property retrievals from optical satellite imagery. For day-time data, these techniques rely on a simultaneous measurement of the cloud reflectance in a non-absorbing (e. g. visible) and absorbing (e. g. near-infrared) wavelengths of the solar spectrum. The reflection of clouds in the visible region is primarily a function of the cloud optical thickness while for the near-infrared region, it is mainly determined by the cloud droplet size (i. e. effective cloud droplet radius). In general, the retrievals can be divided into (i) techniques that use some kind of look-up table (LUT) approach (e. g. Arking and Childs, 1985; Twomey and Cocks, 1989; Nakajima and King, 1990; Han et al., 1994; Nakajima and Nakajima, 1995; Jolivet and Feijt, 2005; King et al., 2004; Roebeling et al., 2006) and (ii) techniques that use a semi-analytical approach (e. g. Kokhanovsky et al., 2003, 2006). The LUT-approaches rely on pre-calculated radiative transfer results based on exact radiative transfer equations that are iteratively lined with actual measured reflectance values. The latter are based on approximate solutions of the asymptotic radiative transfer theory, which can be solved during runtime. Therefore, no time-consuming iterations are necessary.

The significantly increased computation speed associated with the semi-analytical approaches (about factor 50) comes at the expense of the accuracy of the equations used in the retrievals. The error induced by these equations is generally smaller than 5% for satellite zenith angles smaller than 30 and solar zenith angles smaller than 60 degrees which is less than the deviations between different retrieval techniques (e. g. Nauss et al., 2005) or between different sensors (e. g. Roebeling et al., 2006). In addition and more noteworthy, the asymptotic approximations used within that retrievals are only valid for very weakly absorbing media (i. e. single scattering albedo close to 1.0) leading to errors for water and/or ice clouds with large particles in channels with high absorption of light by condense water. Therefore Kokhanovsky and Nauss (2006) have introduced a new forward radiative transfer model (CLOUD) which is based on the asymptotic theory but no longer restricted to a certain range of viewing geometries or weakly absorbing media. CLOUD forms the basis for the new cloud property retrieval SLALOM which is presented in section 2. The accuracy of the new retrieval as compared to both theoretically computed cloud reflectance values and retrieved cloud properties from the

*Corresponding author
Email addresses: thomas.nauss@uni-bayreuth.de (Thomas Nauss), alexk@iup.physik.uni-bremen.de (Alexander A. Kokhanovsky)

NASA MODIS product (MOD06) is discussed in section 3.

2. Theory

The new cloud property retrieval is based on SimpLe Approximations for cLOudy Media (SLALOM) and applicable to a broad variety of optical satellite sensors. Actually, the application is only restricted by the availability of a few look-up tables (see below) computed with respect to the sensor characteristics which can easily be done using the radiative transfer code from Mishchenko et al. (1999) (please do not hesitate to contact the authors for assistance). At the time of publication, look-up tables for Terra-/Aqua-MODIS and Meteosat-SEVIRI are available for download along with the Fortran source codes of the techniques at http://www.klimatologie.uni-bayreuth.de.

As forward model within SLALOM, the CLOUD code is used (Kokhanovsky and Nauss, 2006). Below, the main characteristics of CLOUD will be introduced first since they are necessary for the understanding of SLALOM.

2.1. The forward model: CLOUD

A detailed description of the algorithm used within the forward model CLOUD can be found in Kokhanovsky and Nauss (2006). Therefore, only a brief summary should be given here. To start with, the reflection function of optically thick homogeneous plane-parallel light scattering layers over a Lambertian surface with an albedo A is given by the following analytical form (van de Hulst, 1980; Kokhanovsky and Nauss, 2006)

$$R_A(\mu_0,\mu,\phi) = R(\mu_0,\mu,\phi) + \frac{At_d(\mu_0)t_d(\mu)}{1-Ar_s} \quad (1)$$

with

$$R(\mu_0,\mu,\phi) = R_\infty(\mu_0,\mu,\phi) - T(\mu_0,\mu)le^{-k\tau} \quad (2)$$

and

$$T(\mu_0,\mu) = tn^{-2}K(\mu_0)K(\mu). \quad (3)$$

$$t = \frac{mn^2e^{-k\tau}}{1-l^2e^{-2k\tau}}. \quad (4)$$

Here $R \equiv R_A(A=0)$, $T(\mu_0,\mu)$ is the transmission function for $(A=0)$ with the global transmittance t, $t_d(\mu_0)$ is the diffuse transmittance of a layer under illumination along the direction $\vartheta_0 = arccos(\mu_0)$, r_s is the spherical albedo, τ is the optical thickness, K is the escape function, μ_0 and μ are the cosines of the solar and viewing zenith angles, ϕ is the relative azimuth angle. $R_\infty(\mu_0,\mu,\phi)$ is the reflection function of a semi-infinite scattering layer having the same local optical characteristics as the finite layer under study (i.e. the same single scattering albedo ω and the same phase function $p(\Theta)$ with scattering angle Θ).

The functions r_s and $t_d(\mu)$ are given by

$$r_s = 2\int_0^1 r_p(\mu)\mu\, d\mu \quad (5)$$

$$t_d(\mu) = 2\int_0^1 \overline{T}(\mu_0,\mu)\mu_0\, d\mu_0 \quad (6)$$

with

$$\overline{T}(\mu_0,\mu) = \frac{1}{2\pi}\int_0^{2\pi} T(\mu_0,\mu,\phi)\, d\phi \quad (7)$$

and the spherical albedo $r_p(\mu)$ is defined by

$$r_p(\mu) = 2\int_0^1 \overline{R}(\mu_0,\mu)\mu_0\, d\mu_0 \quad (8)$$

with

$$\overline{R}(\mu_0,\mu) = \frac{1}{2\pi}\int_0^{2\pi} R(\mu_0,\mu,\phi)\, d\phi. \quad (9)$$

Hence, analytical expressions for r_s, t_d and r_p can be derived from Eq. 1 to 4 with account for the definitions in Eq. 5 to 9 by

$$r_s = r_{s\infty} - lte^{-k\tau}, \quad (10)$$

$$t_d(\mu) = tn^{-1}K(\mu) \quad (11)$$

and

$$r_p = r_{p\infty}(\mu) - ltn^{-1}K(\mu)e^{-k\tau}. \quad (12)$$

To use these analytical equations above, the parameters k, l, m, n, $r_{s\infty}$ and also functions $K(\mu)$, $R_\infty(\mu_0,\mu,\phi)$ and $r_{p\infty}(\mu)$ have to be derived. For the non-absorbing case with single scattering albedo $\omega_0 = 1$, they can be defined as $k = m = 0$ and $l = n = r_{s\infty} = r_{p\infty}(\mu) = 1$ but for arbitrary values of ω_0, the parameterizations of van de Hulst (1982) and King and Harshvardhan (1986) have to be used leading to

$$k = \left(\sqrt{3}s - \frac{(0.985-0.253s)s^2}{6.464-5.464s}\right)(1-\omega_0 g) \quad (13)$$

$$l = \frac{(1-s)(1-0.681s)}{1+0.729s} \quad (14)$$

$$m = (1+1.537s)ln\left(\frac{1+1.8s-7.087s^2+4.74s^3}{(1-0.819s)(1-s)^2}\right) \quad (15)$$

$$n = \sqrt{\frac{(1-s)(1+0.414s)}{1+1.888s}} \quad (16)$$

$$r_{s\infty} = \frac{(1-s)(1-0.139s)}{1+1.17s}. \quad (17)$$

The similarity parameter s is defined by

$$s = \sqrt{\frac{1-\omega_0}{1-\omega_0 g}} \quad (18)$$

with the asymmetry parameter g according to

$$g = \frac{1}{4} \int_0^{\pi} p(\theta) sin(2\theta)\, d\theta. \quad (19)$$

In contrast to the just listed parameters, functions $K(\mu)$, $R_\infty(\mu_0, \mu, \phi)$ and $r_{p\infty}(\mu)$ can only be parameterized in terms of the similarity parameter if the application is restricted to values of ω_0 very close to one. The utilization of such parameterizations is the reason why the semi-analytical techniques presented in the introduction fail for arbitrary absorbing media (Kokhanovsky et al., 2003, 2006; Kokhanovsky and Nauss, 2005). Consequently, to avoid this restriction within the new retrieval approach, radiative transfer models of Wauben (1992) and Mishchenko et al. (1999) have been used to compute look-up-tables (LUTs) for these functions for different angles (μ and μ_0 between 0 and 1, ϕ between 0 and 180, step 1) and different values of ω_0 between 0.80 and 1.00 (step 0.01 for $0.80 \leq \omega_0 \leq 0.99$ and 0.001 for $\omega_0 \geq 0.99$). For $R_\infty(\mu_0, \mu, \phi)$, two LUTs have been calculated in order to account for water and ice clouds. For the former a fixed gamma particle size distribution with an effective radius of $10\mu m$ and for the latter a fractal model described by Mishchenko et al. (1999) has been used. Note that due to the reciprocity principle (van de Hulst, 1980), functions $K(\mu)$ and $r_{p\infty}(\mu)$ are identical to $K(\mu_0)$ and $r_{p\infty}(\mu_0)$. In order to account for the difference between the asymmetry parameter used for the computation of the LUTs and the actual value which depends not only on the wavelength but also on the effective cloud droplet radius, the similarity parameter (and not the single scattering albedo) is used for representing the interpolation grid of the LUTs within CLOUD and SLALOM.

Using this approach, the CLOUD model is fast, accurate, and capable to calculate multiple radiative transfer characteristics of cloudy media. For a detailed description and accuracy study please refer to Kokhanovsky and Nauss (2006).

2.2. The inverse model: SLALOM

The retrieval of optical and microphysical cloud properties from daytime satellite data is commonly based on the well-known characteristics of the reflection function in a non-absorbing (visible) and an absorbing (near-infrared) wavelengths. The former is mainly a function of the optical thickness, the latter mainly a function of the effective cloud droplet radius defined by Hansen and Travis (1974) as

$$a_{ef} = \frac{\int_0^{\infty} a^3 f(a) da}{\int_0^{\infty} a^2 f(a)\, da} \quad (20)$$

for the spectrum $f(a)$ of droplets with radii a.

For the present study, the SimpLe Approximations for cLOudy Media (SLALOM) retrieval for the determination of the cloud optical thickness, the effective droplet radius, the liquid and ice water paths as well as the particle absorption length is introduced. Similar to the Semi-Analytical CloUd Retrieval Algorithm (SACURA; Kokhanovsky et al., 2003, 2006), approximated solutions of the radiative transfer theory are used which can easily be solved during runtime. The main and most important difference between SACURA and SLALOM is that the latter is no longer restricted to the case where the probability of absorption $\beta = 1 - \omega_0$ is close to zero. This is due to the substitution of the approximate equations for $K(\mu)$, $R_\infty(\mu_0, \mu, \phi)$ used within SACURA by the tabulated values of these functions within the CLOUD model approach. Note that the LUTs within CLOUD are only used for reading the appropriate function values and not for an iterative retrieval of the cloud properties itself as it is done in the time-consuming procedures of some commonly used LUT retrievals (e. g. Nakajima and Nakajima, 1995; Kawamoto et al., 2001). Therefore, the computation speed of SLALOM is still fully comparable to the very efficient SACURA (Nauss, 2005) and yet it gives more accurate results.

For measurements in a non-absorbing channel (i. e. $0.8\mu m$, index na) it follows from Eq. 1 and 2 with $k = 0.0$ and under consideration of the substitutions given in Section 2.1 that

$$R_{na} = R_\infty - \frac{t(1 - A_{na})}{1 - A_{na}(1 - t)} K_0 K. \quad (21)$$

The global transmittance

$$t = (h + 0.75(1 - g)\tau)^{-1}, \quad (22)$$

(with $h = 1.072$) can be determined for the non-absorbing channel from the measured reflectance R_{na} as

$$t_{na} = [(1 - A_{na})(R_\infty - R_{na})] / [(1 - A_{na})K_0 K - A_{na}(R_\infty - R_{na})]\,. \quad (23)$$

with A_{na} as the underlying surface albedo at the corresponding wavelength. Consequently, Eq. 23 can be used to retrieve the optical thickness in the non-absorbing channel

$$\tau_{na} = \frac{t_{na}^{-1} - h}{0.75(1 - g_{na})} \quad (24)$$

(with t_{na} from Eq. 23 and g_{na} from Eq. A.4, see Appendix A).

After the initial computation of the transmission in the non-absorbing wavelength using Eq. 23, SLALOM starts with the retrieval of the effective cloud droplet radius by computing the reflection function R_{acomp} of the absorbing channel (e. g. $1.6\mu m$, index a). From Section 2.1 it follows that the measured signal R_a in an absorbing channel can be given by

$$R_{acomp} = R_\infty(\mu_0, \mu, \phi) - l t_a n^{-2} K(\mu_0) K(\mu) e^{-k\tau_a} + \frac{A t^2 n^{-2} K(\mu_0) K(\mu)}{1 - A r_s}. \quad (25)$$

The computation of the reflectance R_{acomp} depends on the values of g_a, ω_{0a}, and the cloud optical thickness in the absorbing channel t_a. In order to compute R_{acomp} we use the parameterizations from Kokhanovsky et al. (2003) and Kokhanovsky

and Nauss (2006) to relate these local cloud parameters to the values of a_{ef} and the wavelength independent liquid water path computed via τ_{na} from the readily known t_{na} (see Appendix A).

Therefore,

$$F(a_{ef}) = R_a - R_{acomp} = 0 \tag{26}$$

leads to a single transcendent equation for the determination of the the desired value of a_{ef}. The root of $F(a_{ef})$ can easily be found numerically using Brent's method (Brent, 1973). This iteration is the reason why SLALOM is classified as a *semi-analytical* retrieval. Please note that the speed of the root search is comparable to the speed of the computation speed of any other expression consisting only of ordinary elementary functions.

After the final retrieval of a_{ef} by Brent's method, the cloud optical thickness in the non-absorbing wavelength can be found using Eq. 24, where g is determined via a_{ef} as described in Appendix A.

3. Accuracy of the new retrieval algorithm

Cloud property retrievals are in general validated against theoretically derived datasets or in-situ flight measurements. While the former type of validation shows the range of errors due to the concept or numerical uncertainties of the algorithms the latter in general only allows to make rough assumptions of the retrieval accuracy mainly because of inhomogeneity of cloud fields, different measurement heights (e. g., satellite measurements, in-situ data at mid-level of a cloud, etc.) and sample volumes. Since many different retrievals are used in national and international research projects it is of great importance to study the expected deviations between them. Therefore SLALOM is compared to both theoretical computations from exact radiative transfer models and the well known NASA MODIS MOD06 product (King et al., 1997; Platnick et al., 2003).

3.1. Comparison of SLALOM against exact radiative transfer calculations

In order to theoretically analyze the accuracy of the approximated equations used within the SLALOM retrieval, the reflection of a cloud at $\lambda_{na} = 0.856\mu m$ and $\lambda_a = 1.630\mu m$ was computed using the exact radiative transfer model SCIATRAN (see http://www.iup.uni-bremen.de/sciatran/index.html). Values of τ ranging between 3 and 100 and values of a_{ef} of $6\mu m$, $10\mu m$ and $16\mu m$ and a constant sun zenith angle of 60 have been used. The observation zenith angle was set to 0. The resulting reflection values have been used as input for the SLALOM retrieval.

Figures 1 and 2 show the results for the optical thickness for the three different values of a_{ef}. The results for the effective droplet radius as a function of the optical thickness can be seen in figures 3 and 4 for the same three values of the radius. The deviations for the optical thickness (see figures 1 and 2) are generally smaller than 5 % for τ larger 5. An exception is found for the case of $a_{ef} = 16\mu m$ for which the deviation increases to 9 % if τ reaches 100. The results for the retrieved

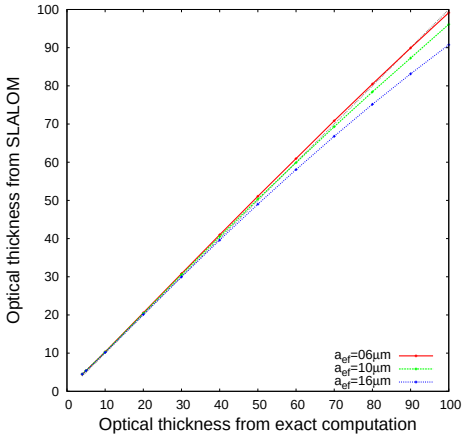

Figure 1: Retrieved optical thickness as a function of the optical thickness used for the exact input computations for three different values of the effective droplet radius.

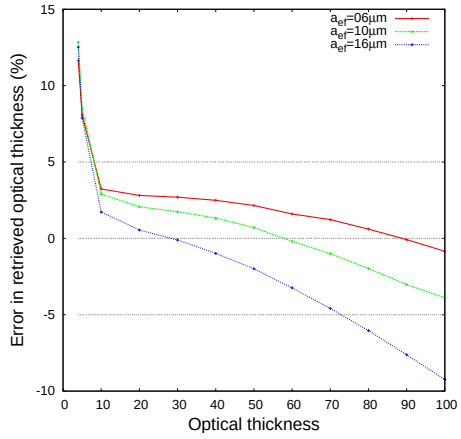

Figure 2: Error of the retrieved optical thickness as a function of the optical thickness used for the exact input computations for three different values of the effective droplet radius.

effective radius (see figures 3 and 4) are of even better quality and the deviation is generally below 2 % to 3 % except for very small τ. Please note that the obvious "best fit" of the results for an a_{ef} value of $10\mu m$ is due to the LUTs used for the SLALOM computation which have been generated for a droplet size of $10\mu m$. However, errors induced by the commonly assumption of plane-parallel homogeneous clouds etc. are much larger than the errors induced by the slight dependence of the retrieval results on the settings used for the computation of the LUTs (Nauss et al., 2005).

In order to give an impression of the error propagation within the retrieval algorithm, the exact SCIATRAN cloud reflectances are modified by 10 % in order to artificially incorporate an error of the measurement. Figure 5 and 6 show the resulting error of the retrieved optical thickness and effective droplet radius. The retrieved optical thickness decreases (increases) with decreasing (increasing) reflection. The opposite is true for the effective

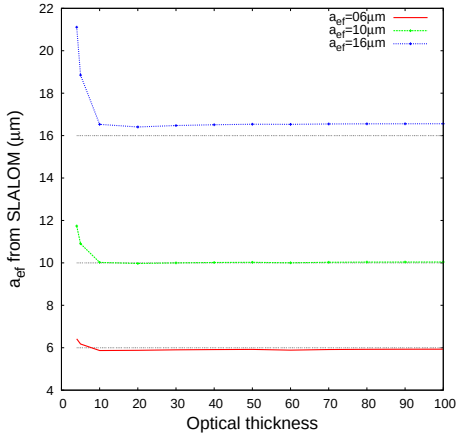

Figure 3: Retrieved effective droplet radius as a function of the optical thickness used for the exact input computations for three different values of the effective droplet radius.

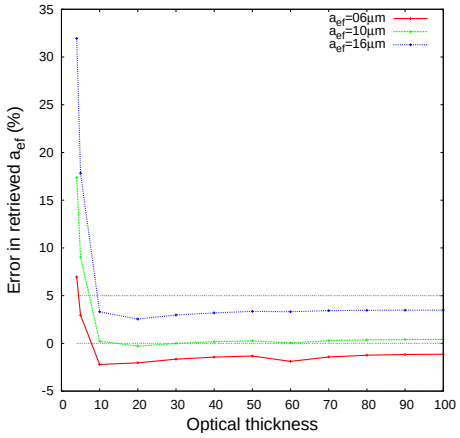

Figure 4: Error of the retrieved effective droplet radius as a function of the optical thickness used for the exact input computations for three different values of the effective droplet radius.

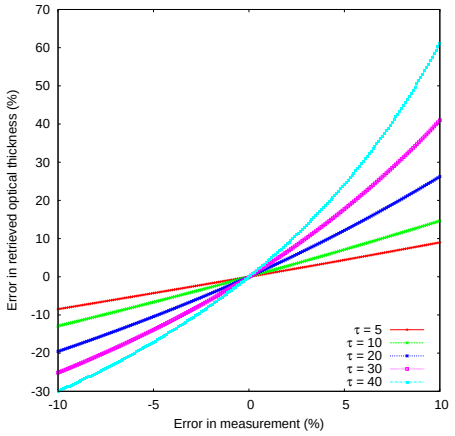

Figure 5: Error of the retrieved optical thickness as a function of an error of the measurement input for different values of the initial optical thickness, an effective droplet radius of 10 μm, a sun zenith angle of 60 and a viewing zenith angle of 0.

droplet radius.

As for the tendency, the resulting errors on the effective droplet radius are generally more linear as compared to the exponential behavior of the error values for the optical thickness. The later is due to the asymptotic behavior of the reflection function of a cloud i. e. uncertainties of the cloud reflectance lead to larger differences of the optical thickness within thick clouds than in thin clouds with a small to medium reflection. For measurement errors of 10 % the retrieval errors increase to about 40 % for the optical thickness (except for large τ) and 30 % for the effective droplet radius. For both parameters the error propagation intensifies for an increasing optical thicknesses.

3.2. Comparison of the inverse algorithm to the MODIS MOD06 product

The theoretical errors discussed in the previous section which result from the approximate equations used within SLALOM do not allow conclusions on the reliability of the retrieval technique alone. This is primarily due to the fact that all commonly used cloud property retrievals are based on the assumption of plane-parallel homogeneous cloud layers. The related errors of the retrieved cloud properties therefore might conceal the intrinsic retrieval errors of SLALOM. For real-world (climate monitoring) applications information on the relative accuracy between SLALOM and other retrievals is consequently much more important. Hence, results from a comparison between SALOM and NASA's MODIS MOD06 product (King et al., 1997; Platnick et al., 2003), a look-up table based approach developed in the framework of the NASA EOS mission (King and Greenstone, 1999), will be presented in this section.

The Terra-MODIS granule from July 18th 2001, 15:30 UTC shown in figure 7 was chosen for the comparison. It covers the west coast of South America and adjacent Pacific areas and was already published by Platnick et al. (2003) and Nauss (2005). The already computed MOD06 product was supplied by NASA's Distributed Active Archive Center (DAAC,

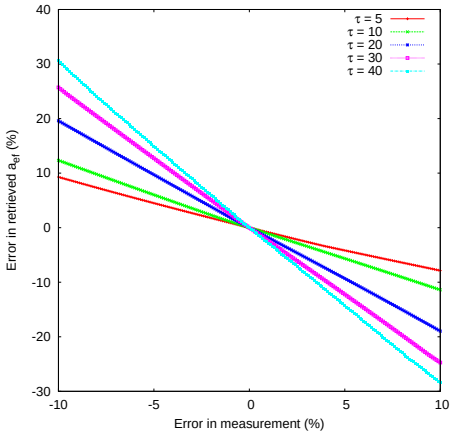

Figure 6: Error of the retrieved effective droplet radius as a function of an error of the measurement input for different values of the initial optical thickness, an effective droplet radius of 10 μm, a sun zenith angle of 60 and a viewing zenith angle of 0.

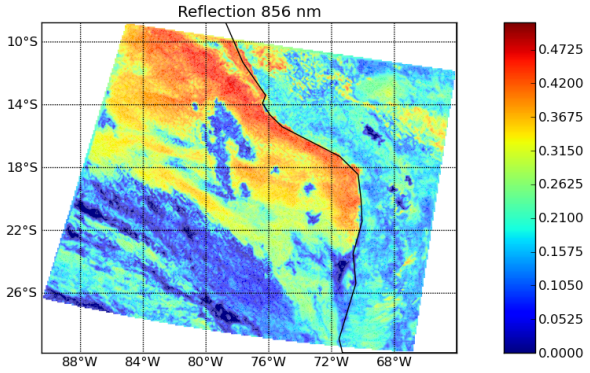

Figure 7: Terra-MODIS granule from July 18th 2001, 15:30 UTC.

http://daac.gsfc.nasa.gov/). Since the 1.6μm channel of MODIS is used for the retrieval of a_{ef}, the analogous MOD06 product and not the standard 2.1μm results is used for the comparison to eliminate errors due to different (wavelength-dependent) penetration depths into the clouds. For the SLALOM retrieval, the corresponding raw data products (MOD01 and MOD03) have also been supplied by DAAC and pre-processed by the authors (Nauss et al., 2005). The satellite and solar zenith angles range between 0 to 65 and 35 to 60 respectively.

The areas in figures 8 and 9 show the field of marine stratocumulus clouds with an optical thickness larger than 10 that are taken into account leading to a test sample ofs over 950.000 pixels each with a resolution of $1km^2$. Thin clouds and clouds over land are not considered for the retrieval since the influence of auxiliary data (e. g. background albedo) should be minimized for this comparison. Please note that for operational retrievals, the background albedo for the actual seen can be supplied on a pixel basis using e. g. the NASA MODIS albedo product for the actual sensor or some kind of minimum composit algorithm for the previous scenes.

The optical thickness retrieved by the two techniques is shown in figure 8a and b respectively with values from 10 to about 73 (not shown in the maps for contrast reasons). The thickest clouds can be found along the coast of Peru, in the center of the scene and along the south-western border of the cloud field. In the center, the small scale inhomogeneities (10 to 30 km across) of the mesoscale cellular convection cumulus cloud tops, further accentuated by 3-D radiation effects can be clearly identified. The mean optical thickness of 17.9 (MOD06) and 17.9 (SLALOM) as well as the median values of 16.6 (MOD06) and 16.8 (SLALOM) are (almost) identical. As shown in figure 8c, the SLALOM retrieved values are slightly larger than the ones from the NASA retrieval. This is consistent with previous comparisons where the NASA retrieval shows the same tendency even if compared to classical LUT-approaches. Both distribution functions have a positive skewness and the standard deviation of the retrieved SLALOM values (5.7) is fully comparable to the NASA retrieval (5.9). The squared correlation coefficient r is 0.99. However and with respect to figure 8d, scattering is generally large for thin clouds but decreases for increasing τ.

The retrieved effective cloud droplet radii are shown in figures 9a and b respectively. Minimum values of a_{ef} are 5μm, maximum values range from 30μm (MOD06) to 37.3μm (SLALOM). As for τ, the largest droplets can be found southwest of an about 200 km wide band along the coast and at the southern border. The large values around the enclosed patches of open cells can be likely traced back to a combination of enhanced 3-D effects, sub-pixel cloudiness and drizzle. Compared to the cloud thickness, the differences of the mean values of the droplet radius (11.0 for MOD06 and 11.5 for SLALOM) are slightly larger and show corresponding standard deviations of 3.2 and 3.4 but the overall correlation with an r^2 of 0.97 is still very good. Again, the SLALOM retrieved values are slightly larger.

It is worth noting that although the resulting cloud parameters between MOD06 and SLALOM show some small differences, the overall agreement is very good. A perfect agreement can not be expected and larger differences have been found even between two look-up table approach retrievals like MOD06 and the Japanese ATSK3 (Nauss, 2005) or between different sensors (Roebeling et al., 2006). The quantity of differences found between SLALOM and MOD06 clearly supports the applicability of SLALOM in operational monitoring projects even though the new retrieval is based on approximated solutions of the radiative transfer equations. The significant increase in computation speed and the undemanding hardware requirements (standard laptops are sufficient to compute a MODIS granule within less than one minute) fully justify the use of the simplified equations even more if spatio-temporal high resolution satellite sensor systems are taken into account.

Please note that we do not present results for the liquid water path, since it is basically just a multiplication of the retrieved optical thickness and cloud droplet values and the comparison

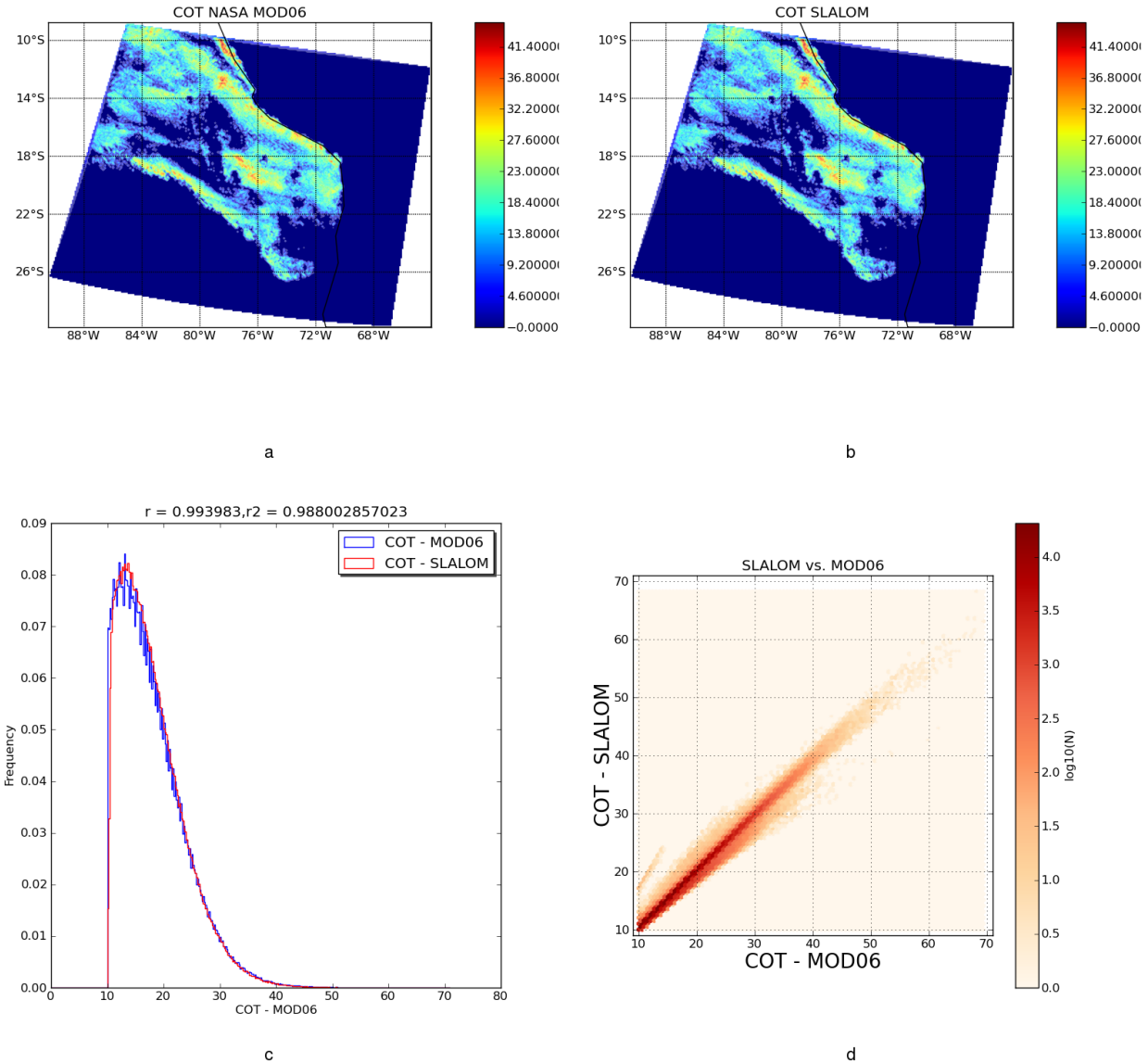

Figure 8: Cloud optical thickness (COT) retrieved by NASA MOD06 (a) and SLALOM (b) for the Terra-MODIS scene from figure 7 as well as corresponding histogram (c) and scatter (d) plots. Numbers above the histogram represent values of the correlation (r) and squared correlatoin coefficient (r^2) between the two datasets.

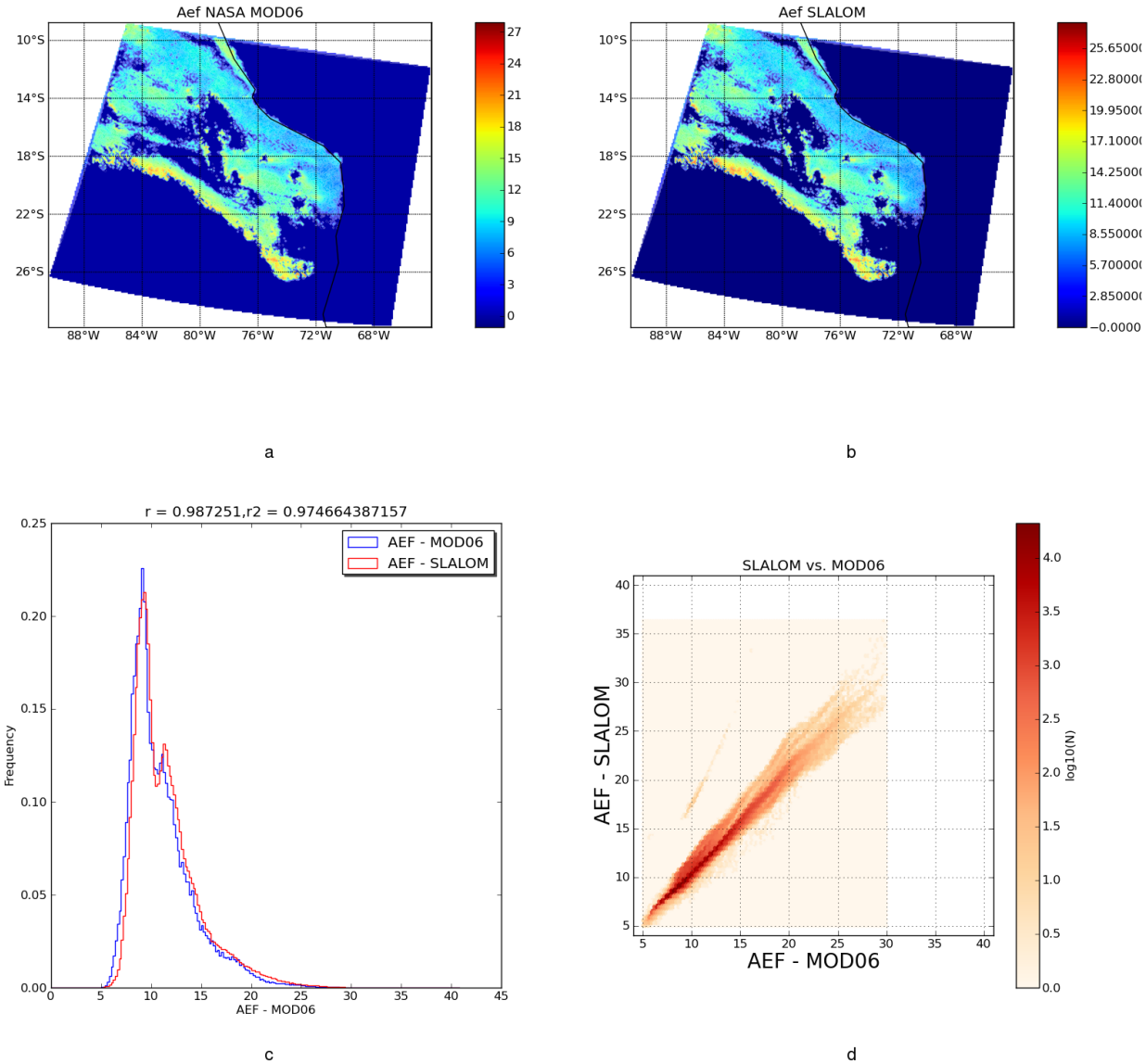

Figure 9: Cloud effective droplet radius ($a_{ef}[\mu m]$) retrieved by NASA MOD06 (a) and SLALOM (b) for the Terra-MODIS scene from figure 7 as well as corresponding histogram (c) and scatter (d) plots. Numbers above the histogram represent values of the correlation (r) and squared correlatoin coefficient (r^2) between the two datasets.

would not lead to new insights into the retrieval accuracy. For the ice cloud retrieval, no comparisons against MODIS products have been performed since differences in the a priori assumption of particle shapes and the vertical profile of the asymmetry parameter would induce considerable discrepancies between the retrievals.

4. Conclusions

A new semi-analytical cloud property retrieval - SLALOM - has been introduced. To retrieve the cloud optical thickness, the effective cloud droplet radius, the particle absorption length and the liquid and ice water paths, SLALOM relies on the simultaneous measurement of the cloud reflection in a non-absorbing (visible) and slightly absorbing (near-infrared) wavelength. But in contrast to the preceding SACURA retrieval (Kokhanovsky et al., 2003; Nauss et al., 2005), SALOM is no longer restricted to the case of single scattering albedos very close to one. This could be achieved by using pre-computed values for the functions of $K(\mu)$ and $R_\infty(\mu_0, \mu, \phi)$ for water and ice clouds as well as for the non-absorbing and absorbing wavelengths. The utilization of the mentioned look-up tables does not mean that SLALOM falls into the "look-up table approach" category of the cloud property retrievals since the inverse problem is solved by approximated analytical equations and not by iterative and time consuming solutions of the inverse problem. This approach enables a very time efficient implementation of the equations leading to fast and hardware undemanding computation speeds.

In order to estimate the accuracy of SLALOM, exact radiative transfer computations have been used as input values and errors in the resulting cloud properties have been analyzed. In general, the errors are very small and well below 5 %. Since SLALOM as well as all commonly used retrievals are based on the assumption of plane-parallel, homogeneous cloud levels, it is much more important to estimate the performance of SLALOM in a real-case situation. Therefore the rather simple SLALOM approach has been compared to the NASA MOD06 product for a scene over the Pacific ocean. The analysis reveals very close and fully comparable results.

Given the accuracy of SLALOM, potential applications are wide spread and beside a stand-alone application it can be used e. g. in the look-up table codes to generate a first guess or to reject unphysical results. It also can be applied for physical insights in the cloud retrieval processes itself and moreover it can be used for other products like e. g. rainfall retrievals.

The retrieval algorithm as described in the paper is valid for warm clouds. Since particles in ice clouds are large and also of nonspherical shapes, SLALOM includes a seperate ice retrieval chain, which is a slight modification of the algorithm described above. In particular, it is assumed that the asymmetry parameter and the cloud optical thickness do not depend on the wavelength. Hence, τ as defined in Eqs. 24 and 25 is used in Eq. 26 without any modification. For the determination of R_∞, LUTs for an ice fractal crystal model haven been computed and the value of g is assumed to be equal 0.75 for such a model (Macke et al., 1996; Mishchenko et al., 1999). The single scattering albedo is then determined from Eq. 26 and provided in the output of the retrieval code. In addition, SLALOM derives the particle absorption length and the effective crystal size using the same model as described above (Kokhanovsky and Nauss, 2005).

A well documented and ready to run FORTRAN implementation (GNU compilers are sufficient) of both the forward CLOUD and the inverse SLALOM model along with all necessary look-up tables is available for download under the Creative Commons Attribution-Noncommercial-Share Alike 3.0 license (see http://creativecommons.org/licenses/by-nc-sa/3.0) at http://www.klimatologie.uni-bayreuth.de.

5. Acknowledgements

We are grateful to M. I. Mishchenko for providing his radiative transfer code valid for a semi-infinite homogeneous light scattering slab and would like to thank NASA for supplying MODIS data. W. M. F. Wauben provided his code for the calculation of the escape function at arbitrary absorption. This is acknowledged with many thanks.

Appendix A. Parameterizations of local optical characteristics

To relate the local cloud parameters g, ω_0 and τ to values of a_{ef} and the liquid water path LWP, we use the parameterizatinos from Kokhanovsky et al. (2003). The single scattering albedo is determined by

$$\omega_0 = 1 - \frac{\sigma_{abs}}{\sigma_{ext}} \tag{A.1}$$

with

$$\sigma_{abs} = \frac{4\pi\chi_{ia}}{\lambda} \sum_{n=0}^{4} d_n \left(\frac{2\pi}{\lambda} a_{ef}\right)^n \tag{A.2}$$

and

$$\sigma_{ext} = \frac{1.5}{a_{ef}} \left(1.0 + 1.1 / \left(\frac{2\pi}{\lambda} a_{ef}\right)^{2/3}\right) \tag{A.3}$$

and the asymmetry parameter is calculated using

$$g = 1 - \sum_{n=0}^{4} c_n \left(\frac{2\pi}{\lambda} a_{ef}\right)^{2n/3}. \tag{A.4}$$

For λ, the wavelength of the non-absorbing or absorbing channels are used respectivley and the imaginary part of the refractive index χ_{ia} is taken from Segelstein (1981) for water and Warren (1984, updates 2008) for ice clouds and the values of c_n, d_n can be found in table A.1 for several wavelengths.

Since the computation of the reflectance R_{acomp} depends on the values of g_a, ω_{0a}, and τ_a in the absorbing channel, we use the parameterizations from Kokhanovsky et al. (2003) and Kokhanovsky and Nauss (2006) to relate these local cloud parameters to the values of a_{ef} and the liquid water path (see Appendix A.

Table A.1: Parameters c and d for different wavelenghts

λ [μm]	c_0	c_1	c_2	c_3	c_4
0.645	0.1121	0.5118	0.8997	0.0	0.0
0.859	0.1115	0.4513	1.2719	0.0	0.0
1.630	0.0608	2.465	-32.98	248.94	-636.0
λ [μm]	d_0	d_1	d_2	d_3	d_4
1.630	1.671	0.0025	-2.365E-4	2.861E-6	-1.05E-8

To compute the cloud reflectance in the absorbing channel R_{acomp} and solve Eq. 26, the value of the cloud optical thickness for the same wavelength τ_a must be available. Since only τ_{na} can be computed at this stage of the retrieval using Eq. 24 with the transmission t_{na} determined from Eq. 23, the wavelength independent liquid water path (LWP) is used. The latter is defined by

$$LWP = C_v D \rho \tag{A.5}$$

~~with the volumetric droplet concentration C_v and the geometrical cloud thickness D and~~ can be expressed in terms of τ_{na} using

$$LWP = \tau_{na} \rho a_{ef} / 1.5 \left(1 + 1.1 / \left(\frac{2\pi}{\lambda_{na}} a_{ef} \right)^{2/3} \right)^{-1} . \tag{A.6}$$

with λ_{na} as the wavelength of the non-absorbing channel ~~and ρ as the density of water~~ (see Kokhanovsky et al., 2003). Finally, τ_a can be derived by

$$\tau_a = \frac{1.5 LWP}{\rho a_{ef}} \left(1 + 1.1 / \left(\frac{2\pi}{\lambda_a} a_{ef} \right)^{2/3} \right) \tag{A.7}$$

and used in Eq. 25 to finally solve Eq. 26.

References

Arking, A., Childs, J.D., 1985. Retrieval of cloud cover parameters from multispectral satellite images. Journal of Applied Meteorology 24, 322–333.

Brent, R.P.C., 1973. 3-4 in Algorithms for minimization without derivatives. Prentice-Hall.

Han, Q., Rossow, W.B., Lacis, A.A., 1994. Near-global survey of effective droplet radii in liquid water clouds using isccp data. Journal of Climate 7, 465–497.

Hansen, J.E., Travis, L.D., 1974. Light scattering in planetary atmospheres. Space Science Reviews 16, 527–610.

Houghton, J.T., Ding, Y., Griggs, D.J., Noguer, M., van der Linden, P.J., Dai, X., Maskel, K., Johnson, C.A. (Eds.), 2001. Climate Change 2001: The Scientific Basis. Cambridge University Press, Cambridge, UK.

van de Hulst, H.C., 1980. Multiple light scattering: tables, formulas and applications. Academic Press.

van de Hulst, H.C., 1982. Ligth scattering by small particles. Dover Publications.

Jolivet, D., Feijt, A.J., 2005. Quantification of the accuracy of liquid water path fields derived from noaa 16 advanced very high resolution radiometer over three ground stations using microwave radiometers. Journal Of Geophysical Research-Atmospheres 110, D11204.

Kawamoto, K., Nakajima, T., Nakajima, T.Y., 2001. A global determination of cloud microphysics with AVHRR remote sensing. Journal of Climate 14, 2054–2068.

King, M.D., Greenstone, R., 1999. 1999 EOS Reference Handbook. Technical Report NASA NP-1999-08-134-GSFC. Goddard Space Flight Center, Greenbelt, MD.

King, M.D., Harshvardhan, 1986. Comparitive accuracy of selected multiple scattering approximations. Journal of the Atmospheric Sciences 43, 784–801.

King, M.D., Platnick, S., Yang, P., Arnold, G.T., Gray, M.A., Ri?di, J.C., Ackerman, S.A., Liou, K.N., 2004. Remote sensing of liquid water and ice cloud optical thickness, and effective radius in the arctic: Application of airborne multispectral mas data. Journal of Atmospheric and Ocean Technology 21, 857–875.

King, M.D., Tsay, S.C., Platnick, S.E., Wang, M., Liou, K.N., 1997. Cloud retrieval algorithms for MODIS: Optical thickness, effective particle radius, and thermodynamic phase. Algorithm Theoretical Basis Document ATBD-MOD-05. NASA.

Kokhanovsky, A.A., Nauss, T., 2005. Satellite-based retrieval of ice cloud properties using a semi-analytical algorithm. Journal of Geophysical Research - Atmospheres 110/D19, D19206, 10.1029/2004JD005744.

Kokhanovsky, A.A., Nauss, T., 2006. Reflection and transmission of solar light by clouds: asymptotic theory. Atmospheric Chemistry And Physics 6, 5537–5545.

Kokhanovsky, A.A., Rozanov, V.V., Nauss, T., Reudenbach, C., Daniel, J.S., Miller, H.L., Burrows, J.P., 2006. The semianalytical cloud retrieval algorithm for SCIAMACHY – I. The validation. Atmospheric Chemistry and Physics 6, 1905–1911.

Kokhanovsky, A.A., Rozanov, V.V., Zege, E.P., Bovensmann, H., Burrows, J.P., 2003. A semianalytical cloud retrieval algorithm using backscattered radiation in 0.4–2.4 μm spectral region. Journal of Geophysical Research 108, AAC 4–1–AAC 4–19.

Kühnlein, M., Thies, B., Nauss, T., Bendix, J., 2010. Rainfall rate assignment using msg-seviri data-a promising approach to space-born rain rate retrieval for mid latitudes. Journal of Applied Meteorology and Climatology (accepted) .

Lensky, I.M., Rosenfeld, D., 2006. The time-space exchangeability of satellite retrieved relations between cloud top temperature and particle effective radius. Atmospheric Chemistry And Physics 6, 2887–2894.

Macke, A., Mueller, J., Raschke, E., 1996. Scattering properties of atmospheric ice crystals. Journal of the Atmospheric Sciences 53, 2813–2825.

Mishchenko, M.I., Dlugach, J.M., Yanovitskij, E.G., Zakharova, N.T., 1999. Bidirectional reflectance of flat, optically thick particulate layers: An efficient radiative transfer solution and applications to snow and soil surfaces. Journal of Quantitative Spectroscopy and Radiative Transfer 63, 409–432.

Nakajima, T., King, M.D., 1990. Determination of the optical thickness and effective particle radius of clouds from reflected solar radiation measurements. part I: Theory. Journal of the Atmospheric Sciences 47, 1878–1893.

Nakajima, T.Y., Nakajima, T., 1995. Wide-area determination of cloud microphysical properties from NOAA AVHRR measurements for FIRE and ASTEX regions. Journal of the Atmospheric Sciences 52, 4043–4059.

Nauss, T., 2005. Das Rain Area Delineation Scheme RADS – Ein neues Verfahrens zur satellitengestützten Erfassung der Niederschlagsfläche über Mitteleuropa. Phd thesis. Fachbereich Geographie, Universität Marburg.

Nauss, T., Kokhanovsky, A.A., 2006. Discriminating raining from non-raining clouds at mid-latitudes using multispectral satellite data. Atmospheric Chemistry And Physics 6, 5031–5036.

Nauss, T., Kokhanovsky, A.A., 2007. Assignment of rainfall confidence values using multispectral satellite data at mid-latitudes: first results. Advances in Geosciences 10, 99–102.

Nauss, T., Kokhanovsky, A.A., Nakajima, T.Y., Reudenbach, C., Bendix, J., 2005. The intercomparison of selected cloud retrieval algorithms. Atmospheric Research 78, 46–78.

Platnick, S., King, M.D., Ackerman, S.A., Menzel, W.P., Baum, B.A., Riédi, J.C., Frey, R.A., 2003. The MODIS cloud products: Algorithms and examples from Terra. IEEE Transactions on Geoscience and Remote Sensing 41, 459–473.

Platnick, S., Valero, F.P.J., 1995. A validation of a satellite cloud retrieval during astex. Journal of the Atmospheric Sciences 52, 2985–3001.

Roebeling, R.A., Feijt, A.J., Stammes, P., 2006. Cloud property retrievals for climate monitoring: Implications of differences between spinning enhanced visible and infrared imager (seviri) on meteosat-8 and advanced very high resolution radiometer (avhrr) on noaa-17. Journal Of Geophysical Research-Atmospheres 111, D20210.

Roebeling, R.A., Holleman, I., 2009. Seviri rainfall retrieval and validation using weather radar observations. Journal Of Geophysical Research-Atmospheres 114, D21202.

606 Segelstein, D.J., 1981. The complex refractive index of water. M.S. thesis.
607 University of Missouri – Kansas City, Department of Physics.
608 Thies, B., Nauss, T., Bendix, J., 2008. Precipitation process and rain-
609 fall intensity differentiation using meteosat second generation spinning en-
610 hanced visible and infrared imager data. Journal Of Geophysical Research-
611 Atmospheres 113, D23206.
612 Twomey, S., Cocks, T., 1989. Remotes sensing of cloud parameters from spec-
613 tral reflectance in the near-infrared. Beiträge zur Physik der Atmosphäre 62,
614 172–179.
615 Warren, S.G., 1984. Optical constants of ice from the ultraviolet to the mi-
616 crowave. Applied Optics 23, 1026–1225.
617 Wauben, W.M.F., 1992. Multiple Scattering of Polarized Radiation in Planetary
618 Atmospheres. Ph.D. thesis. Free University of Amsterdam.